Linear magnetoresistance on the topological surface

C. M. Wang[1,*] and X. L. Lei[2]

[1]*School of Physics and Electrical Engineering, Anyang Normal University, Anyang 455000, China*

[2]*Department of Physics, Shanghai Jiaotong University, 1954 Huashan Road, Shanghai 200030, China*

(Received 15 March 2012; revised manuscript received 25 June 2012; published 26 July 2012)

A positive, nonsaturating, and dominantly linear magnetoresistance is demonstrated to occur in the surface state of a topological insulator having a wave-vector linear energy dispersion together with a finite positive Zeeman energy splitting. This linear magnetoresistance shows up within quite wide magnetic-field range in a spatially homogeneous system of high carrier density and low mobility in which the conduction electrons are in extended states and spread over many smeared Landau levels, and is robust against increasing temperature, in agreement with recent experimental findings in Bi_2Se_3 nanoribbons.

DOI: 10.1103/PhysRevB.86.035442 PACS number(s): 75.47.−m, 73.20.At, 73.25.+i

I. INTRODUCTION

It is well known that the classical magnetoresistance (MR) in metals or semiconductors with a closed free-electron Fermi surface increases quadratically with increasing magnetic field B for $\mu B \ll 1$ and saturates when $\mu B > 1$. Here, μ is the zero-magnetic-field mobility. Hence, the extraordinarily high and linear MR (LMR), which breaks this familiar rule, has been gaining much attention as soon as its discovery. In the past decade, this unexpected LMR has been reported in silver chalcogenide,[1] indium antimonide,[2] silicon,[3] MnAs-GaAs composite material,[4] and graphene.[5]

Kapitza's linear law[6] indicates that the metal shows a magnetoresistance linear in perpendicular magnetic field when it has an open Fermi surface and a mean-free path longer than the electronic Larmor radius. Recently, another two models, irrespective of the open Fermi surface, have been constructed to provide possible mechanisms for the LMR phenomenon. Abrikosov suggested a quantum-limit origin of LMR for the homogeneous system with a gapless linear energy spectrum.[7,8] His model requires that Landau levels are well formed and the carrier concentration is small so that all electrons occupy only the lowest Landau band. Alternatively, Parish and Littlewood developed a classical model without involving linear spectrum.[9] Ignoring the concrete microscopic mechanism, they attributed this unusual MR to the mobility fluctuations in a strongly inhomogeneous system.

Topological insulators[10–12] (TIs) are novel materials with a full energy gap in bulk, while there are gapless surface states. Due to its unique band structure with only one helical Dirac cone and linear energy dispersion,[13–15] the surface states of the TI Bi_2Se_3 become an excellent platform for the study of quantum-limit LMR. The recent experiment in this flat surface system, however, reported that a large positive MR, which becomes very linear above a characteristic field of $1 \sim 2$ T, was observed even in an opposite situation where the carrier-sheet density is high so that electrons occupy more than one Landau level.[16] Moreover, they found that raising temperature to room temperature almost has no influence on the observed LMR. It is striking that this observation is in conflict with Abrikosov's model and also with the classical Parish-Littlewood model. So far, a reliable theoretical scheme capable of explaining this novel experiment has still been lacking.

In this paper, we generalize the balance-equation approach[17] to a system modeling the surface states of a three-dimensional TI to investigate the two-dimensional magnetotransport in it. We find that a positive, nonsaturating, and dominantly linear magnetoresistance can appear within quite wide magnetic-field range in the TI surface state having a positive and finite effective g factor. This linear magnetoresistance shows up in the system of high carrier concentration and low mobility when electrons are in extended states and spread over many smeared Landau levels, and persists up to room temperature, providing a possible mechanism for the recently observed linear magnetoresistance in topological-insulator Bi_2Se_3 nanoribbons.[16]

II. BALANCE-EQUATION FORMULATION FOR MAGNETORESISTIVITY

We consider the surface state of a Bi_2Se_3-type large bulk gap TI in the x-y plane under the influence of a uniform magnetic field $\boldsymbol{B}$ applied along the z direction.[15] Following the experimental observation,[16] we assume that the Fermi energy locates in the gap of the bulk band and above the Dirac point, i.e., the surface carriers are electrons. Further, the separations of the Fermi energy from the bottom of bulk band and Dirac point are much larger than the highest temperature (300 K) considered in this work. Hence, the contribution from the bulk band to the magnetotransport is negligible. These electrons, scattered by randomly distributed impurities and by phonons, are driven by a uniform in-plane electric field $\boldsymbol{E} = (E_x, E_y)$ in the topological surface. The Hamiltonian of this many-electron and phonon system consists of an electron part $\mathcal{H}_{\rm e}$, a phonon part $\mathcal{H}_{\rm ph}$, and electron-impurity and electron-phonon interactions $\mathcal{H}_{\rm ei}$ and $\mathcal{H}_{\rm ep}$:

$$\mathcal{H} = \mathcal{H}_{\rm e} + \mathcal{H}_{\rm ei} + \mathcal{H}_{\rm ep} + \mathcal{H}_{\rm ph}. \tag{1}$$

Here, the electron Hamiltonian is taken in the form

$$\mathcal{H}_{\rm e} = \sum_j \left[v_{\rm F}\left(\pi_j^x \sigma_j^y - \pi_j^y \sigma_j^x\right) + \frac{1}{2} g_z \mu_{\rm B} B \sigma_j^z + e\boldsymbol{r}_j \cdot \boldsymbol{E} \right], \tag{2}$$

in which $\boldsymbol{\pi}_j \equiv \boldsymbol{p}_j + e\boldsymbol{A}(\boldsymbol{r}_j) = (\pi_j^x, \pi_j^y)$, $\boldsymbol{r}_j = (x_j, y_j)$, $\boldsymbol{p}_j = (p_{jx}, p_{jy})$, and $\boldsymbol{\sigma}_j = (\sigma_j^x, \sigma_j^y, \sigma_j^z)$ stand, respectively, for the canonical momentum, coordinate, momentum, and spin operators of the jth electron having charge $-e$, $\boldsymbol{A}(\boldsymbol{r}) = (-By, 0)$

is the vector potential of the perpendicular magnetic field $\boldsymbol{B} = B\hat{z}$ in the Landau gauge, $v_{\rm F}$ is the Fermi velocity, g_z is the effective g factor of the surface electron, and $\mu_{\rm B} = e/2m_0$ is the Bohr magneton with m_0 the free-electron mass. The sum index j in Eq. (2) goes over all electrons of total number N in the surface state of unit area.

In the framework of the balance-equation approach,[17–19] the two-dimensional center-of-mass (c.m.) momentum and coordinate $\boldsymbol{P} = \sum_j \boldsymbol{p}_j$ and $\boldsymbol{R} = N^{-1}\sum_j \boldsymbol{r}_j$, and the relative-electron momenta and coordinates $\boldsymbol{p}'_j = \boldsymbol{p}_j - \boldsymbol{P}/N$ and $\boldsymbol{r}'_j = \boldsymbol{r}_j - \boldsymbol{R}$ are introduced to write the Hamiltonian $\mathcal{H}_{\rm e}$ into the sum of a single-particle c.m. part $\mathcal{H}_{\rm cm}$ and a many-particle relative-electron part $\mathcal{H}_{\rm er}$: $\mathcal{H}_{\rm e} = \mathcal{H}_{\rm cm} + \mathcal{H}_{\rm er}$, with

$$\mathcal{H}_{\rm cm} = v_{\rm F}\big(\Pi_x\sigma_{\rm c}^y - \Pi_y\sigma_{\rm c}^x\big) + NeE\cdot R, \tag{3}$$

$$\mathcal{H}_{\rm er} = \sum_j\left[v_{\rm F}\big(\pi_j'^x\sigma_j^y - \pi_j'^y\sigma_j^x\big) + \frac{1}{2}g_z\mu_{\rm B}B\sigma_j^z\right]. \tag{4}$$

In this, $\boldsymbol{\Pi} \equiv \boldsymbol{P} + NeA(\boldsymbol{R}) = (\Pi_x,\Pi_y)$ is the canonical momentum of the center of mass and $\boldsymbol{\pi}'_j \equiv \boldsymbol{p}'_j + eA(\boldsymbol{r}'_j) = (\pi_j'^x,\pi_j'^y)$ is the canonical momentum for the jth relative electron. Here, we have also introduced c.m. spin operators $\sigma_{\rm c}^x \equiv N^{-1}\sum_j\sigma_j^x$ and $\sigma_{\rm c}^y \equiv N^{-1}\sum_j\sigma_j^y$. The commutation relations between the c.m. spin operators $\sigma_{\rm c}^x$ and $\sigma_{\rm c}^y$ and the spin operators σ_j^x,σ_j^y, and σ_j^z of the jth electron are of order of $1/N$: $[\sigma_j^{\beta_1},\sigma_{\rm c}^{\beta_2}] = N^{-1}2\,{\rm i}\,\varepsilon_{\beta_1\beta_2\beta_3}\sigma_j^{\beta_3}$ with $\beta_1,\beta_2,\beta_3 = (x,y,z)$. Therefore, for a macroscopic large-N system, the c.m. part $\mathcal{H}_{\rm cm}$ actually commutes with the relative-electron part $\mathcal{H}_{\rm er}$ in the Hamiltonian, i.e., the c.m. motion and the relative motion of electrons are truly separated from each other. The couplings between the two emerge only through the electron-impurity and electron-phonon interactions. Furthermore, the electric field $\boldsymbol{E}$ shows up only in $\mathcal{H}_{\rm cm}$. And, in view of $[r'_{i\alpha},p'_{j\beta}] = {\rm i}\delta_{\alpha\beta}(\delta_{ij} - 1/N) \simeq {\rm i}\delta_{\alpha\beta}\delta_{ij}$, i.e., the relative-electron momenta and coordinates can be treated as canonical conjugate variables, the relative-motion part $\mathcal{H}_{\rm er}$ is just the Hamiltonian of N electrons in the surface state of TI in the magnetic field without the presence of the electric field.

In terms of the c.m. coordinate $\boldsymbol{R}$ and the relative-electron density operator $\rho_{\boldsymbol{q}} = \sum_j e^{{\rm i}\boldsymbol{q}\cdot\boldsymbol{r}'_j}$, the electron-impurity and electron-phonon interactions can be written as[18,19]

$$\mathcal{H}_{\rm ei} = \sum_{\boldsymbol{q},a} U(\boldsymbol{q})\,e^{{\rm i}\boldsymbol{q}\cdot(\boldsymbol{R}-\boldsymbol{r}_a)}\rho_{\boldsymbol{q}}, \tag{5}$$

$$\mathcal{H}_{\rm ep} = \sum_{\boldsymbol{Q},\lambda} M(\boldsymbol{Q},\lambda)\,\phi_{\boldsymbol{Q}\lambda}e^{{\rm i}\boldsymbol{q}\cdot\boldsymbol{R}}\rho_{\boldsymbol{q}}. \tag{6}$$

Here, $U(\boldsymbol{q})$ and $M(\boldsymbol{Q},\lambda)$ are, respectively, the impurity potential (an impurity at randomly distributed position $\boldsymbol{r}_a$) and electron-phonon coupling matrix element in the plane-wave representation, and $\phi_{\boldsymbol{Q}\lambda} \equiv b_{\boldsymbol{Q}\lambda} + b^\dagger_{-\boldsymbol{Q}\lambda}$ with $b^\dagger_{\boldsymbol{Q}\lambda}$ and $b_{\boldsymbol{Q}\lambda}$ being the creation and annihilation operators for a phonon of wave vector $\boldsymbol{Q} = (\boldsymbol{q},q_z)$ in branch λ having frequency $\Omega_{\boldsymbol{Q}\lambda}$.

The c.m. velocity (operator) $\boldsymbol{V}$ is the time variation of its coordinate: $\boldsymbol{V} = \dot{\boldsymbol{R}} = -{\rm i}[\boldsymbol{R},\mathcal{H}] = v_{\rm F}(\sigma_{\rm c}^y\,\hat{i} - \sigma_{\rm c}^x\,\hat{j})$. To derive a force-balance equation for steady-state transport, we consider the Heisenberg equation for the rate of change of the c.m. canonical momentum $\boldsymbol{\Pi}$:

$$\dot{\boldsymbol{\Pi}} = -{\rm i}\,[\boldsymbol{\Pi},\mathcal{H}] = -Ne(\boldsymbol{V}\times\boldsymbol{B}) - NeE + \boldsymbol{F}_{\rm i} + \boldsymbol{F}_{\rm p}, \tag{7}$$

in which the frictional forces $\boldsymbol{F}_{\rm i}$ and $\boldsymbol{F}_{\rm p}$ share the same expressions as given in Ref. 19.

The statistical average of the operator equation (7) can be determined to linear order in the electron-impurity and electron-phonon interactions $\mathcal{H}_{\rm ei}$ and $\mathcal{H}_{\rm ep}$ with the initial density matrix $\hat{\rho}_0 = Z^{-1}e^{-(\mathcal{H}_{\rm ph}+\mathcal{H}_{\rm er})/T}$ at temperature T when the in-plane electric field $\boldsymbol{E}$ is not strong. For steady-transport states we have $\langle\dot{\boldsymbol{\Pi}}\rangle = 0$, leading to a force-balance equation of the form

$$0 = -Ne\boldsymbol{v}\times\boldsymbol{B} - NeE + \boldsymbol{f}_{\rm i} + \boldsymbol{f}_{\rm p}. \tag{8}$$

Here, $\boldsymbol{v} = \langle\boldsymbol{V}\rangle$, the statistically averaged velocity of the moving center of mass, is identified as the average rate of change of its position, i.e., the drift velocity of the electron system driven by the electric field $\boldsymbol{E}$, and $\boldsymbol{f}_{\rm i}$ and $\boldsymbol{f}_{\rm p}$ are frictional forces experienced by the center of mass due to impurity and phonon scatterings:

$$\boldsymbol{f}_{\rm i} = \sum_{\boldsymbol{q}}|U(\boldsymbol{q})|^2\boldsymbol{q}\,\Pi_2(\boldsymbol{q},\omega_0), \tag{9}$$

$$\boldsymbol{f}_{\rm p} = \sum_{\boldsymbol{Q},\lambda}|M(\boldsymbol{Q},\lambda)|^2\boldsymbol{q}\,\Pi_2(\boldsymbol{q},\Omega_{\boldsymbol{Q}\lambda}+\omega_0) \times\left[n\left(\frac{\Omega_{\boldsymbol{Q}\lambda}}{T}\right) - n\left(\frac{\Omega_{\boldsymbol{Q}\lambda}+\omega_0}{T}\right)\right], \tag{10}$$

in which $n(x) = (e^x-1)^{-1}$ is the Bose distribution function, $\omega_0 \equiv \boldsymbol{q}\cdot\boldsymbol{v}$, and $\Pi_2(\boldsymbol{q},\omega)$ stands for the imaginary part of the Fourier spectrum of the relative-electron density correlation function defined by

$$\Pi(\boldsymbol{q},t-t') = -{\rm i}\,\theta(t-t')\langle[\rho_{\boldsymbol{q}}(t),\rho_{-\boldsymbol{q}}(t')]\rangle_0, \tag{11}$$

where $\rho_{\boldsymbol{q}}(t) = e^{{\rm i}\mathcal{H}_{\rm er}t}\rho_{\boldsymbol{q}}\,e^{-{\rm i}\mathcal{H}_{\rm er}t}$ and $\langle\cdots\rangle_0$ denotes the statistical averaging over the initial density matrix $\hat{\rho}_0$.[17]

The force-balance equation (8) describes the steady-state two-dimensional magnetotransport in the surface state of a TI. Note that the frictional forces $\boldsymbol{f}_{\rm i}$ and $\boldsymbol{f}_{\rm p}$ are in the opposite direction of the drift velocity $\boldsymbol{v}$ and their magnitudes are functions of $v = |\boldsymbol{v}|$ only. With the drift velocity $\boldsymbol{v} = (v,0)$ in the x direction, the force-balance equation (8) yields a transverse resistivity $R_{xy} = -E_y/(Nev) = -B/(Ne)$, and a longitudinal resistivity $R_{xx} = -E_x/(Nev) = -(f_{\rm i}+f_{\rm p})/(N^2e^2v)$. The linear one is in the form

$$R_{xx} = -\frac{1}{N^2e^2}\sum_{\boldsymbol{q}}|U(\boldsymbol{q})|^2q_x^2\frac{\partial}{\partial\omega}\Pi_2(\boldsymbol{q},\omega)\big|_{\omega=0} - \frac{1}{2TN^2e^2}\sum_{\boldsymbol{Q},\lambda}|M(\boldsymbol{Q},\lambda)|^2q_x^2\Pi_2(\boldsymbol{q},\Omega_{\boldsymbol{Q}\lambda}) \times{\rm csch}^2\left(\frac{\Omega_{\boldsymbol{Q}\lambda}}{2T}\right). \tag{12}$$

III. DENSITY CORRELATION FUNCTION IN THE LANDAU REPRESENTATION

For calculating the electron density correlation function $\Pi_2(\boldsymbol{q},\omega)$, we proceed in the Landau representation.[19,20] The Landau levels of the single-particle Hamiltonian $h = v_{\rm F}(\pi^x\sigma^y - \pi^y\sigma^x) + \frac{1}{2}g_z\mu_{\rm B}B\sigma^z$ of the relative-electron system in the absence of electric field are composed of a positive ("+") and a negative ("−") branch[21–25]

$$\varepsilon_n^{\pm} = \pm\sqrt{2n\varepsilon_s^2 + \delta_z^2} = \pm\varepsilon_n \quad (n = 1,2,\ldots) \tag{13}$$

with $\varepsilon_s = v_F\sqrt{eB}$ and $\delta_z = -\frac{1}{2}g_z\mu_{\rm B}B$, and a zero ($n = 0$) level

$$\varepsilon_0 = \delta_z = -\tfrac{1}{2}g_z\mu_{\rm B}B. \tag{14}$$

The corresponding Landau wave functions are

$$\Psi^+_{n,k_x}(\boldsymbol{r}) = \frac{1}{\sqrt{\mathcal{R}_n}}e^{ik_x x}\begin{pmatrix} i\mathcal{P}_{\rm n}\phi_{\rm n-1,k_x}(y) \\ \phi_{n,k_x}(y)\end{pmatrix} \tag{15}$$

and

$$\Psi^-_{n,k_x}(\boldsymbol{r}) = \frac{1}{\sqrt{\mathcal{R}_n}}e^{ik_x x}\begin{pmatrix} \phi_{n-1,k_x}(y) \\ i\mathcal{P}_n\phi_{n,k_x}(y)\end{pmatrix} \tag{16}$$

for $n = 1,2,\ldots$; and

$$\Psi_{0,k_x}(\boldsymbol{r}) = e^{{\rm i}k_x x}\begin{pmatrix} 0 \\ \phi_{0,k_x}(y)\end{pmatrix} \tag{17}$$

for $n = 0$. Here, k_x is the wave vector of the system along the x direction; $\mathcal{R}_n = 1 + \mathcal{P}_n^2$ with $\mathcal{P}_n = \sqrt{2n}\varepsilon_s/(\delta_z + \sqrt{2n\varepsilon_s^2 + \delta_z^2})$; and $\phi_{n,k_x}(y) = D_n\exp(-\gamma^2/2)H_n(\gamma)$ is the harmonic-oscillator eigenfunction with $H_n(x)$ being the Hermite polynomial, $\gamma \equiv (y - y_c)/l_{\rm B} = \sqrt{eB}(y - k_x l_{\rm B}^2)$, and $D_n = 1/(2^n n!)^{1/2}(eB/\pi)^{1/4}$.

Each Landau level contains $n_{\rm B} = eB/2\pi = 1/(2\pi l_{\rm B}^2)$ electron states for a system of unit surface area. The positive branch $\varepsilon_n^+ = \varepsilon_n$ and the $n = 0$ level ε_0 of the above energy spectra are indeed quite close to those of the surface states in the bulk gap of Bi_2Se_3-family materials derived from microscopic band calculation.[15]

The Landau levels are broadened due to impurity, phonon, and electron-electron scatterings. We model the imaginary part of the retarded Green's function, or the density of states, of the broadened Landau level n (written for "+" branch and $n = 0$ levels), using a Gaussian-type form[26]

$${\rm Im}G_n(\epsilon) = -\frac{\sqrt{2\pi}}{\Gamma}\exp\left[-\frac{2(\epsilon - \varepsilon_n)^2}{\Gamma^2}\right], \tag{18}$$

with a half-width Γ of the form[22] $\Gamma = [2\omega_c/(\pi\tau_s)]^{1/2}$. Here, τ_s is the single-particle lifetime and $\omega_c = eBv_{\rm F}^2/\varepsilon_{\rm F}^0$ is the cyclotron frequency of linear-energy-dispersion system with $\varepsilon_{\rm F}^0 = 2v_{\rm F}\sqrt{\pi N}$ being the zero-temperature Fermi level. Using a semiempirical parameter α to relate τ_s with the transport scattering time $\tau_{\rm tr} = 4\alpha\tau_s$, and expressing $\tau_{\rm tr}$ with the zero-field mobility μ at finite temperature,[27] we can write the Landau-level broadening as

$$\Gamma = (ev_{\rm F}/\pi)[2B\alpha/(N\mu)]^{1/2}. \tag{19}$$

In this study, we consider the case of n doping, i.e. the Fermi level is high enough above the energy zero of the Dirac cone in the range of "+"-branch levels and the states of "−"-branch levels are completely filled, that they are irrelevant to electron transport.

Special attention has to be paid to the $n = 0$ level since, depending on the direction of exchange potential, the effective g factor of a TI surface state g_z can be positive, zero, or negative.[24,25] The sign and magnitude of the effective g factor determines how many states of the zero level should be included in or excluded from the available states for electron occupation in the case of n doping at a magnetic field. (i) If $g_z = 0$, the $n = 0$ level center is exactly at $\varepsilon_0 = 0$ and the system is electron-hole symmetric. The total number of negative energy states (including the states of the lower half of the $n = 0$ level and states of the "−"-branch levels) and that of positive energy states (including the states of the upper half of the $n = 0$ level and states of the "+"-branch levels) do not change when changing magnetic field. Therefore, the lower-half negative energy states of this level are always filled and the upper-half positive-energy states of it are available for the occupation of particles, which are counted as electrons participating in transport in the case of n doping. (ii) For a finite positive $g_z > 0$, the $n = 0$ level ε_0 moves downward to negative energy and its distance to the nearest "−"-branch level is $2|\delta_z| = g_z\mu_{\rm B}B$ closer than to the nearest "+"-branch level at finite magnetic-field strength B. This is equivalent to the opening of an increasingly enlarged (with increasing B) energy gap between the "+"-branch states and the states of the zero-level and the "−"-branch levels. The opening of a sufficient energy gap implies that with increasing magnetic field, the states in the "+"-branch levels would no longer shrink into the zero level, and thus the $n = 0$ level should be completely excluded from the conduction band, i.e., only particles occupying the "+"-branch states are counted as electrons participating in transport in the case of n doping, when the magnetic field B gets larger than a certain value (depending on the magnitude of g_z). (iii) For a finite negative $g_z < 0$, the $n = 0$ level ε_0 moves upward to positive energy and an increasingly enlarged energy gap will be opened between the states of the zero-level and the "+" branch and the states of "−"-branch levels, and particles occupying the $n = 0$ level and "+"-branch states are electrons participating in transport when the magnetic field B gets larger than a certain value.

As a result, the experimentally accessible sheet density N of electrons participating in transport is related to the Fermi energy $\varepsilon_{\rm F}$ by the following equation valid at finite g_z for the magnetic field B larger than a certain value:

$$N = -\frac{1}{2(\pi l_{\rm B})^2}\int d\epsilon\, f(\epsilon)\sum_n^{\infty}{\rm Im}G_n(\epsilon), \tag{20}$$

in which $f(\epsilon) = \{\exp[(\epsilon - \varepsilon_{\rm F})/T] + 1\}^{-1}$ is the Fermi distribution function at temperature T and the summation index n goes over $(1,2,\ldots)$ for $g_z > 0$, or $(0,1,2,\ldots)$ for $g_z < 0$. In the case of $g_z = 0$,

$$N = -\frac{1}{2(\pi l_{\rm B})^2}\int d\epsilon\, f(\epsilon)\left[\sum_{n=1}^{\infty}{\rm Im}G_n(\epsilon) + {\rm Im}G_0^p(\epsilon)\right] \tag{21}$$

valid for arbitrary magnetic field, in which $\mathrm{Im}G_0^p(\epsilon) = \mathrm{Im}G_0(\epsilon)\theta(\epsilon)$.

The imaginary part of relative-electron density correlation function in the presence of a magnetic field $\Pi_2(\boldsymbol{q},\omega)$ can be expressed in the Landau representation as[19,20]

$$\Pi_2(\boldsymbol{q},\omega) = \frac{1}{2\pi l_B^2}\sum_{n,n'} C_{n,n'}\left(l_B^2 q^2/2\right)\Pi_2(n,n',\omega), \quad (22)$$

in which the transform factor

$$C_{n,n'}(\xi) \equiv \frac{e^{-\xi}\xi^{n_2-n_1}}{\mathcal{R}_n\mathcal{R}_{n'}}\frac{n_1!}{n_2!}\Bigg[L_{n_1}^{n_2-n_1}(\xi) + s_n s_{n'}\mathcal{P}_n\mathcal{P}_{n'}\sqrt{\frac{n_2}{n_1}}L_{n_1-1}^{n_2-n_1}(\xi)\Bigg]^2, \quad (23)$$

with $n_1 = \min(n,n')$, $n_2 = \max(n,n')$, $s_n = 1-\delta_{n,0}$, and $L_n^m(x)$ being associated Laguerre polynomials. The Landau-representation correlation function $\Pi_2(n,n',\omega)$ in Eq. (22) can be constructed with the imaginary part of the retarded Green's function $\mathrm{Im}G_n(\epsilon)$, or the density of states, of the nth Landau level as[19,20]

$$\Pi_2(n,n',\omega) = -\frac{1}{\pi}\int d\epsilon[f(\epsilon)-f(\epsilon+\omega)] \times \mathrm{Im}G_n(\epsilon+\omega)\mathrm{Im}G_{n'}(\epsilon). \quad (24)$$

The summation indices n and n' in Eq. (22) are taken over $(1,2,\ldots)$ for $g_z > 0$, or $(0,1,2,\ldots)$ for $g_z < 0$. In the case of $g_z = 0$, Eq. (22) still works and the summation indices n and n' go over $(0,1,2,\ldots)$, but with $\mathrm{Im}G_0(\epsilon)$ replaced by $\mathrm{Im}G_0^p(\epsilon)$ in Eq. (24).

IV. NUMERICAL RESULTS AND DISCUSSIONS

Numerical calculations are performed for the magnetoresistivity R_{xx} of surface state in a uniform TI Bi_2Se_3. At zero temperature, the elastic scattering contributing to the resistivity is modeled by a Coulomb potential due to charged impurities:[28,29] $U(\boldsymbol{q}) = n_i e^2/(2\epsilon_0\kappa q)$ with n_i being the impurity density, which is determined by the zero-magnetic-field mobility μ. At temperatures higher than 50 K,[16] phonon scatterings play an increasingly important role and the dominant inelastic contribution comes from optical phonons. For this polar material, the scattering by optical phonons via the deformation potential can be neglected. Hence, we take account of inelastic scattering from optical phonons via Fröhlich coupling: $|M(\boldsymbol{Q})|^2 = e^2\Omega/(2\epsilon_0 Q^2)(\kappa_\infty^{-1}-\kappa^{-1})$. In the numerical calculation, we use the following parameters:[15,29–31] Fermi velocity $v_F = 5.0\times10^5$ m/s, static dielectric constant $\kappa = 100$, optical dielectric constant $\kappa_\infty = 20$, and phonon energy $\Omega = 7.4$ meV. The broadening parameter is taken to be $\alpha = 3$.

Figure 1 shows the calculated magnetoresistivity R_{xx} versus the magnetic field strength B for a TI surface system with electron sheet density $N = 1.3\times10^{12}$ cm^{-2}, but having different effective g factors: $g_z = 0,10$, and -10 for two values of zero-magnetic-field mobility $\mu = 0.2$ m^2/Vs and $\mu = 0.7$ m^2/Vs, representing different degrees of Landau-level broadening. In the case without Zeeman splitting ($g_z = 0$), the resistivity R_{xx} exhibits almost no change with changing

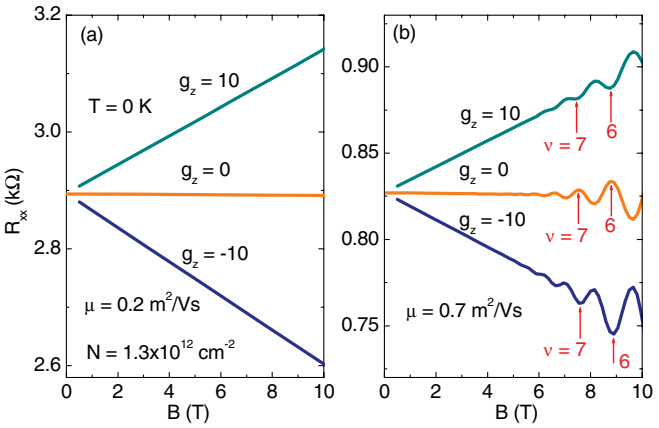

FIG. 1. (Color online) The calculated resistivity R_{xx} as a function of the magnetic field B having different effective g factors: $g_z = 0,10$, and -10 for a TI surface system with electron sheet density $N = 1.3\times10^{12}$ cm^{-2} in the cases of zero-magnetic-field mobility $\mu = 0.2$ m^2/Vs (a) and $\mu = 0.7$ m^2/Vs (b). Several integer-number positions of filling factor $\nu = 2\pi N/(eB)$ are marked in (b).

magnetic field up to 10 T, except the Shubnikov–de Haas (SdH) oscillation showing up in the case of $\mu = 0.7$ m^2/Vs. This kind of magnetoresistance behavior was indeed seen experimentally in the electron-hole symmetrical massless system of single-layer graphene.[32] In the case of a positive g factor, $g_z = 10$, the magnetoresistivity increases linearly with increasing magnetic field, while for a negative g factor, $g_z = -10$, the magnetoresistivity decreases linearly with increasing magnetic field.

In the following, we will give more detailed examination on the linearly increasing magnetoresistance in the positive g_z case. Figure 2 shows the calculated resistivity R_{xx} versus the magnetic-field strength B at lattice temperature $T = 0$ K for system of carrier sheet density $N = 1.3\times10^{12}$ cm^{-2} and $g_z = 10$, having different zero-field mobility $\mu = 0.2,0.35,0.5,0.65,0.8$, and 5 m^2/Vs. All resistivity curves for mobility $\mu \leqslant 0.8$ m^2/Vs exhibit clear linearity in the magnetic-field range and appear to have no tendency of saturation at the highest field shown in the figure. Especially, for the case $\mu = 0.2$ m^2/Vs, the linear behavior extends even up to the magnetic field of 30 T, as illustrated in the inset of Fig. 2(a). This feature contradicts the classical MR which saturates at sufficiently large magnetic field $B \gg \mu^{-1}$.

Note that here we only present the calculated R_{xx} for magnetic field B larger than $B_c = 1$ T, for which a sufficient energy gap $2|\delta_z| = g_z\mu_B B$ is assumed to open that, with further increase of the magnetic field, the states in the "+"-branch levels no longer shrink into the zero level and thus it should be excluded from the conduction band. This is of course not true for very weak magnetic field. When $B \to 0$, the energy gap $2|\delta_z| \to 0$, the situation becomes similar to the case of $g_z = 0$: the whole upper half of the zero-level states are available to electron occupation and we should have a flat resistivity R_{xx} when changing magnetic field. With increasing B, the portion of the zero-level states available to conduction electrons decreases until the magnetic field reaches B_c. As a result, the resistivity R_{xx} should exhibit a crossover from a flat

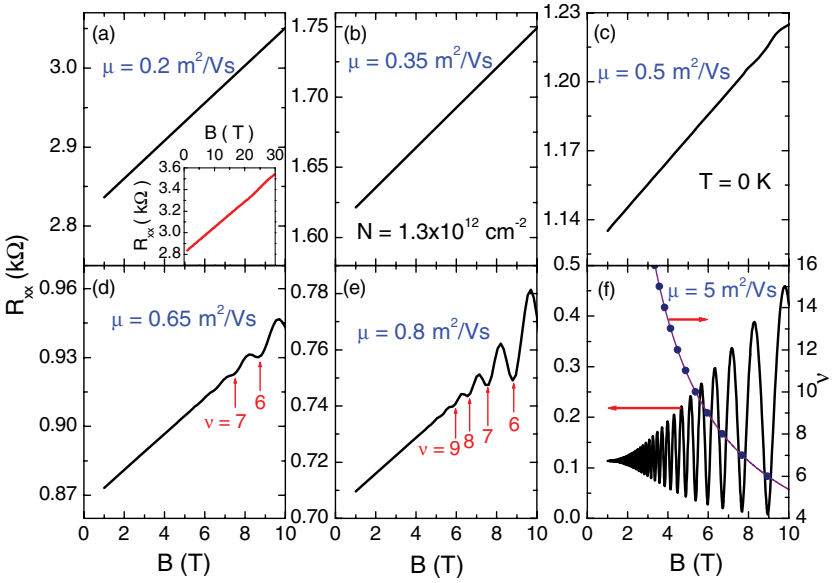

FIG. 2. (Color online) The longitudinal resistivity R_{xx} is shown as a function of the magnetic field B for different values of zero-magnetic-field mobility: (a) $\mu = 0.2$, (b) 0.35, (c) 0.5, (d) 0.65, (e) 0.8, and (f) 5 m^2/Vs. The inset of (a) illustrates the same for a larger magnetic-field range $0 < B < 30$ T. The filling factor ν is plotted versus the magnetic field in (f); and several integer-number positions of ν are also marked in (d) and (e). Here, the surface electron density $N = 1.3 \times 10^{12}\,cm^{-2}$ and the lattice temperature $T = 0$ K.

changing at small B to positively linear increasing at $B > B_c$. This is just the behavior observed in the TI Bi_2Se_3.[16]

Note that in the case of $\mu = 0.2$ m^2/Vs, the broadened Landau-level widths are always larger than the neighboring level interval: $2\Gamma \gtrsim \Delta\varepsilon_n = \varepsilon_{n+1} - \varepsilon_n$, which requires $\mu \lesssim (4e\alpha/N)[(\sqrt{n+1} + \sqrt{n})/\pi]^2$, even for the lowest Landau level $n = 1$, i.e., the whole Landau-level spectrum is smeared. With increasing the zero-field mobility, the magnitude of resistivity R_{xx} decreases, and when the broadened Landau-level width becomes smaller than the neighboring level interval $2\Gamma \lesssim \Delta\varepsilon_n$, a weak SdH oscillation begins to occur around the linearly dependent average value of R_{xx} at higher portion of the magnetic-field range, as seen in Figs. 2(c)–2(e) for $\mu = 0.5$,0.65, and 0.8 m^2/Vs. On the other hand, in the case of large mobility, e.g., $\mu = 5$ m^2/Vs, where the broadened Landau-level widths 2Γ are much smaller than the neighboring level interval even for level index n as large as 30, the magnetoresistivity shows pronounced SdH oscillation and the linear-dependent behavior disappears, before the appearance of quantum Hall effect,[22,33,34] as shown in Fig. 2(f).

Abrikosov's model for the LMR requires the applied magnetic field large enough to reach the quantum limit at which all the carriers are within the lowest Landau level,[7] while it is obvious that more than one Landau level is occupied in the experimental samples in the field range in which the linear and nonsaturating magnetoresistivity was observed.[16] For the given electron surface density $N = 1.3 \times 10^{12}\,cm^{-2}$, the number of occupied Landau levels, or the filling factor $\nu = 2\pi N/(eB)$, at different magnetic fields is shown in Fig. 2(f), as well as in the Figs. 2(d) and 2(e), where the integer-number positions of ν, i.e., filling up to entire ν Landau levels, coincide with the minima of the density of states or the dips of SdH oscillation. This is in contrast with the $g_z = 0$ case, where the integer number of ν, which implies a filling up to the center position of the νth Landau levels, locates at a peak of SdH oscillation, as shown in Fig. 1(b). The observed SdH oscillations in the Bi_2Se_3 nanoribbon exhibiting nonsaturating surface LMR in the experiment[16] favor the former case: a finite positive effective $g_z > 0$.

Next, we examine the density dependence of the linear magnetoresistivity. To compare with Abrikosov's quantum magnetoresistance, which suggests a $R_{xx} \propto N^{-2}$ behavior,[7,35] we show the calculated $R_{xx}N^2$ for the above LMR versus the carrier-sheet density N in Fig. 3 at fixed magnetic field $B = 3$ T. The mobility is taken respectively to be $\mu = 0.2$,0.3,0.4,0.5, and 0.6 m^2/Vs to make the resistivity in the LMR regime. A clearly linear dependence of $R_{xx}N^2$ on the surface density N is seen in all cases, indicating that this nonsaturating linear resistivity is almost inversely proportional to the carrier density. In the figure, we also show $R_{xx}N^2$ versus N under the condition of different given conductivity $\sigma = Ne\mu = 10,13,16$, and $20\,e^2/h$. In this case, the half-width Γ is independent of surface density. The linear dependence still holds, indicating that this linear behavior is not sensitive to the modest N dependence of Landau-level

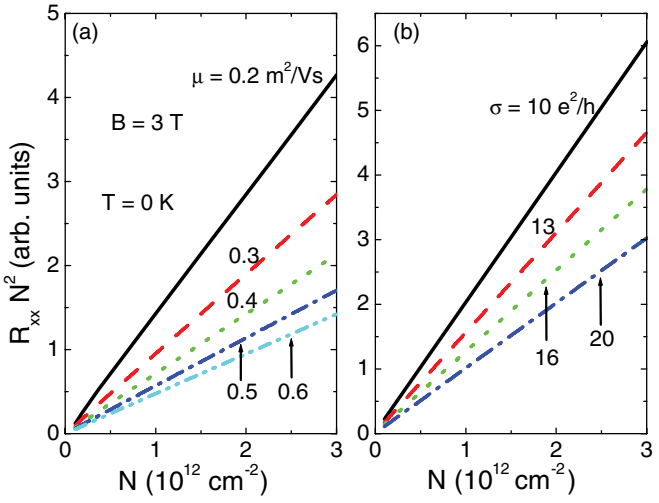

FIG. 3. (Color online) $R_{xx}N^2$ is plotted as a function of the surface electron density N at magnetic field $B = 3$ T: (a) at different values of zero-field mobility μ, and (b) at different values of zero-field conductivity σ.

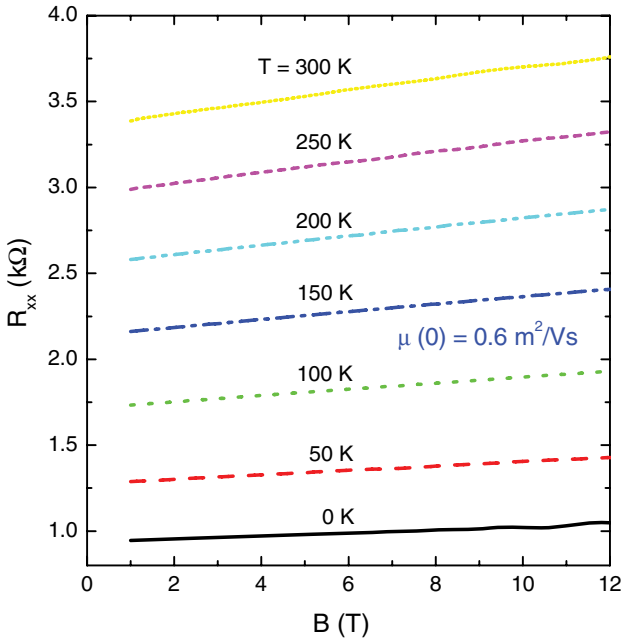

FIG. 4. (Color online) The longitudinal resistivity of the surface state of a TI versus magnetic field B at various lattice temperatures. Here, the zero-magnetic-field mobility at zero temperature is $\mu(0) = 0.6\ \mathrm{m}^2/\mathrm{Vs}$.

broadening Γ as long as the system is in the overlapped Landau-level regime.

From the above discussion, it is obvious that LMR shows up in the system having overlapped Landau levels, and the separation of Landau levels makes the MR departure from the linear increase. At high temperature, the thermal energy would smear the level separation, and phonon scatterings further broaden Landau levels. Hence, it is believed that this LMR will be robust against raising temperature. This is indeed the case as seen in Fig. 4, where we plot the calculated magnetoresistivity R_{xx} for the above system with zero-temperature linear mobility $\mu(0) = 0.6\ \mathrm{m}^2/\mathrm{Vs}$ versus the magnetic field at different lattice temperatures. We can see that raising temperature to room temperature has little effect on the linearity of MR. Due to the decreased mobility at higher temperature from phonon scattering, the weak SdH oscillation on the linear background tends to vanish. These features are in good agreement with the experimental report.[16]

V. SUMMARY

In summary, we have studied the two-dimensional magnetotransport in the flat surface of a three-dimensional TI, which arises from the surface states with a wave-vector linear energy dispersion and a finite, positive Zeeman splitting within the bulk energy gap. When the level broadening is comparable to or larger than the Landau-level separation and the conduction electrons spread over many Landau levels, a positive, dominantly linear, and nonsaturating magnetoresistance appears within a quite wide range of magnetic field and persists up to room temperature. This remarkable LMR provides a possible mechanism for the recently observed linear magnetoresistance in topological insulator Bi_2Se_3 nanoribbons.[16]

In contrast to quantum Hall effect, which appears in the case of well-formed Landau levels and to Abrikosov's quantum magnetotransport,[7,8] which is limited to the extreme quantum limit that all electrons coalesce into the lowest Landau level, the discussed LMR is a phenomenon of pure classical two-dimensional magnetotransport in a system having linear energy dispersion, appearing in the regime of overlapped Landau levels, irrespective of its showing up in relatively high magnetic-field range. Furthermore, the present scheme deals with spatially uniform case without invoking the mobility fluctuation in a strongly inhomogeneous system, which is required in the classical Parish and Littlewood model to produce a LMR.[9]

The appearance of this significant positive-increasing linear magnetoresistance depends on the existence of a positive and sizable effective g factor. If the Zeeman energy splitting is quite small, the resistivity R_{xx} would exhibit little change with changing magnetic field. In the case of a negative and sizable effective g factor, the magnetoresistivity would decrease linearly with increasing magnetic field. Therefore, the behavior of the longitudinal resistivity versus magnetic field may provide a useful way for judging the direction and the size of the effective Zeeman energy splitting in TI surface states.

ACKNOWLEDGMENTS

This work was supported by the National Science Foundation of China (Grant No. 11104002), the National Basic Research Program of China (Grant No. 2012CB927403), and by the Program for Science & Technology Innovation Talents in Universities of Henan Province (Grant No. 2012HASTIT029).

*cmwangsjtu@gmail.com

[1] R. Xu, A. Husmann, T. F. Rosenbaum, M. L. Saboungi, J. E. Enderby, and P. B. Littlewood, Nature (London) **390**, 57 (1997).
[2] J. Hu and T. Rosenbaum, Nat. Mater. **7**, 697 (2008).
[3] M. P. Delmo, S. Yamamoto, S. Kasai, T. Ono, and K. Kobayashi, Nature (London) **457**, 1112 (2009).
[4] H. G. Johnson, S. P. Bennett, R. Barua, L. H. Lewis, and D. Heiman, Phys. Rev. B **82**, 085202 (2010).
[5] A. L. Friedman, J. L. Tedesco, P. M. Campbell, J. C. Culbertson, E. Aifer, F. K. Perkins, R. L. Myers-Ward, J. K. Hite, C. R. Eddy Jr, G. G. Jernigan, and D. K. Gaskill, Nano Lett. **10**, 3962 (2010).
[6] P. L. Kapitza, Proc. R. Soc. A **123**, 292 (1929).
[7] A. A. Abrikosov, Phys. Rev. B **58**, 2788 (1998).
[8] A. A. Abrikosov, Europhys. Lett. **49**, 789 (2000).
[9] M. M. Parish and P. B. Littlewood, Nature (London) **426**, 162 (2003).
[10] C. L. Kane and E. J. Mele, Phys. Rev. Lett. **95**, 226801 (2005).
[11] M. Z. Hasan and C. L. Kane, Rev. Mod. Phys. **82**, 3045 (2010).
[12] X. L. Qi and S. C. Zhang, Rev. Mod. Phys. **83**, 1057 (2011).

[13]Y. Xia, D. Qian, D. Hsieh, L. Wray, A. Pal, H. Lin, A. Bansil, D. Grauer, Y. S. Hor, R. J. Cava, and M. Z. Hasan, Nat. Phys. **5**, 398 (2009).
[14]H. J. Zhang, C. X. Liu, X. L. Qi, X. Dai, Z. Fang, and S. C. Zhang, Nat. Phys. **5**, 438 (2009).
[15]C. X. Liu, X. L. Qi, H. J. Zhang, X. Dai, Z. Fang, and S. C. Zhang, Phys. Rev. B **82**, 045122 (2010).
[16]H. Tang, D. Liang, R. L. J. Qiu, and X. P. A. Gao, ACS Nano **5**, 7510 (2011).
[17]X. L. Lei and C. S. Ting, Phys. Rev. B **30**, 4809 (1984); **32**, 1112 (1985).
[18]X. L. Lei, J. L. Birman, and C. S. Ting, J. Appl. Phys. **58**, 2270 (1985).
[19]W. Cai, X. L. Lei, and C. S. Ting, Phys. Rev. B **31**, 4070 (1985); X. L. Lei, W. Cai, and C. S. Ting, J. Phys. C: Solid State **18**, 4315 (1985).
[20]C. S. Ting, S. C. Ying, and J. J. Quinn, Phys. Rev. B **16**, 5394 (1977).
[21]J. W. McClure, Phys. Rev. **104**, 666 (1956).
[22]Y. Zheng and T. Ando, Phys. Rev. B **65**, 245420 (2002).
[23]M. Zarea and S. E. Ulloa, Phys. Rev. B **72**, 085342 (2005).
[24]Z. G. Wang, Z. G. Fu, S. X. Wang, and P. Zhang, Phys. Rev. B **82**, 085429 (2010).
[25]A. A. Taskin and Y. Ando, Phys. Rev. B **84**, 035301 (2011).
[26]T. Ando, A. B. Fowler, and F. Stern, Rev. Mod. Phys. **54**, 437 (1982).
[27]X. L. Lei and S. Y. Liu, Phys. Rev. Lett. **91**, 226805 (2003).
[28]C. M. Wang and F. J. Yu, Phys. Rev. B **84**, 155440 (2011).
[29]D. Culcer, E. H. Hwang, T. D. Stanescu, and S. Das Sarma, Phys. Rev. B **82**, 155457 (2010).
[30]O. Madelung, *Semiconductors: Data Handbook* (Springer, Berlin, 2004).
[31]X. Zhu, L. Santos, R. Sankar, S. Chikara, C. Howard, F. C. Chou, C. Chamon, and M. El-Batanouny, Phys. Rev. Lett. **107**, 186102 (2011).
[32]Z. B. Tan, C. L. Tan, L. Ma, G. T. Liu, L. Lu, and C. L. Yang, Phys. Rev. B **84**, 115429 (2011).
[33]Y. Zhang, Y. Tan, H. Stormer, and P. Kim, Nature (London) **438**, 201 (2005).
[34]V. P. Gusynin and S. G. Sharapov, Phys. Rev. Lett. **95**, 146801 (2005).
[35]A. A. Abrikosov, J. Phys. A: Math. Gen. **36**, 9119 (2003).